particles

MDPI

Article

Nonleptonic Decays of Doubly Charmed Baryons

Mikhail A. Ivanov

Bogoliubov Laboratory of Theoretical Physics, Joint Institute for Nuclear Research, Dubna 141980, Russia; ivanovm@theor.jinr.ru

Received: 6 January 2020; Accepted: 5 February 2020; Published: 19 February 2020

Abstract: In this lecture, we provide a basic introduction into the topic of charmed baryons and their nonleptonic two-body decays. Some features of the baryon weak decays on the quark level are discussed in detail in the framework of effective field theory. The calculation of the matrix elements of the four-quark operators arising in the effective theory proceeds by using the covariant constituent quark model. The model allows one to evaluate not only the factorizing tree-level diagrams but also more complicated diagrams with the internal W–exchange. The technique required for such calculation is discussed in some detail. Finally, the numerical results are presented, and comparison of the contributions coming from the W–exchange diagrams with those from the tree-level are carefully performed.

Keywords: doubly charmed baryons; covariant constituent quark model; nonleptonic decays

1. Introduction

In 1964, Gell–Mann proposed [1] the theory of quarks–fundamental particles that make up most ordinary matter. It was done by using the observation that the successful eightfold way of hadron classification would be naturally explained if hadrons were composed of a quark-antiquark pair or three quarks (or three antiquarks).

In the same year, George Zweig came to the same conclusion independently [2,3] by analyzing the suppressed strong decays of the ϕ-meson. He called three constituents by aces.

The existence of a fourth quark was discussed by a number of authors around 1964, for instance, by James Bjorken and Sheldon Glashow [4]. But there was little evidence for its existence. Its prediction is usually credited to Glashow–Iliopoulos–Maiani [5] for the so-called GIM mechanism, which forbids the flavor-changing neutral currents in the tree diagrams. It explains why weak interactions that change strangeness by a factor of 2 are suppressed. The first particle containing the charmed quark and antiquark was discovered in 1974 and named as the J/ψ meson.

The masses of singly charmed baryons was predicted in one gluon exchange model developed in Reference [6]. The comprehensive review on heavy baryons, their spectroscopy, and semileptonic and nonleptonic decays may be found in Reference [7]. In Tables 1 and 2, we display the names and quark contents of the low-lying multiplets of charmed baryons with spin $1/2$ and $3/2$, respectively. The values of masses with errors are taken from PDG [8], whereas without errors from Reference [7].

Table 1. Charmed $1/2^+$ baryon states. Notation $[a,b]$ and $\{a,b\}$ for antisymmetric and symmetric flavor index combinations. The third column shows which SU(3) adjoint (*) or fundamental representation the quark state belongs to.

Title	Quark Content	$SU(3)$	(I, I_3)	Mass (MeV)
Λ_c^+	$c[ud]$	3 *	(0,0)	2286.46 ± 0.14
z' Ξ_c^+	$c[us]$	3 *	(1/2,1/2)	2467.93 ± 0.18
Ξ_c^0	$c[ds]$	3 *	(1/2,–1/2)	2470.91 ± 0.25
Σ_c^{++}	cuu	6	(1,1)	2453.97 ± 0.14
Σ_c^+	$c\{ud\}$	6	(1,0)	2452.9 ± 0.4
Σ_c^0	cdd	6	(1,–1)	2453.75 ± 0.14
$\Xi_c'^+$	$c\{us\}$	6	(1/2,1/2)	2578.4 ± 0.5
$\Xi_c'^0$	$c\{ds\}$	6	(1/2,–1/2)	2579.2 ± 0.5
Ω_c^0	css	6	(0,0)	2695.2 ± 1.7
Ξ_{cc}^{++}	ucc	3	(1/2,1/2)	3621.2 ± 0.7
Ξ_{cc}^+	dcc	3	(1/2,–1/2)	3610
Ω_{cc}^+	scc	3	(0,0)	3710

Table 2. Charmed $3/2^+$ baryon states.

Title	Quark Content	$SU(3)$	(I, I_3)	Mass (MeV)
Σ_c^{*++}	cuu	6	(1,1)	2518.41 ± 0.20
Σ_c^{*+}	cud	6	(1,0)	2517.5 ± 2.3
Σ_c^{*0}	cdd	6	(1,–1)	2518.48 ± 0.20
Ξ_c^{*+}	cus	6	(1/2,1/2)	2645.57 ± 0.26
Ξ_c^{*0}	cds	6	(1/2,–1/2)	2646.38 ± 0.21
Ω_c^{*0}	css	6	(0,0)	2765.9 ± 2.0
Ξ_{cc}^{*++}	ucc	3	(1/2,1/2)	3680
Ξ_{cc}^{*+}	dcc	3	(1/2,–1/2)	3680
Ω_{cc}^{*+}	scc	3	(0,0)	3760
Ω_{ccc}^{*++}	ccc	1	(0,0)	4730

The lowest lying multiplet of charmed baryons with spin 1/2 can decay only weakly. Therefore, the study of the nonleptonic decays of charmed baryons is very important in the phenomenology of particle interactions. There are now more precise results on the branching ratios of the two-body decays of charmed baryons $\Lambda_c^+ \to p\phi, \Lambda\pi^+, \Sigma^+\pi^0$ [9] and $\Xi_c^+ \to p\bar{K}^*(892)^o$ [10,11]. In 2005, a new era began in the studies of doubly charmed baryons when the SELEX Collaboration reported on the observation of a state with the quantum numbers of the spin 1/2 ground state Ξ_{cc}^+ baryon with a mass of 3518 ± 3 MeV [12]. The SELEX (Segmented Large X baryon Spectrometer) is a fixed target experiment at Fermilab. This doubly charmed baryon state was conjectured to be an isospin-$\frac{1}{2}$ baryon with quark content (dcc) and to have an isospin partner Ξ_{cc}^{++} with the quark structure (ucc). However, other Collaborations (*BABAR*, Belle, LHCb [8]) found no evidence for the Ξ_{cc}^+ nor the Ξ_{cc}^{++} states in the conjectured mass region of ~ 3500 MeV. Recently, the LHCb Collaboration discovered the doubly charmed state Ξ_{cc}^{++} [13–15] in the invariant mass spectrum of the final state particles $(\Lambda_c^+ K^- \pi^+ \pi^+)$. The LHCb is Large Hadron Collider beauty experiment at CERN. The extracted mass of the Ξ_{cc}^{++} state was given as $3621.40 \pm 0.72 \pm 0.27 \pm 0.14$ MeV and was ~ 100 MeV heavier than the mass of the original SELEX doubly charmed baryon state Ξ_{cc}^+, which made it quite unlikely that the two states were isospin partners. On the other hand, the LHCb mass measurement was in agreement with theoretical mass value predictions for the doubly charmed baryon states. In particular, the central mass value of the LHCb result for the Ξ_{cc}^{++} was very close the value 3610 MeV and 3620 MeV predicted in Reference [7,16] using the one gluon exchange model of de Rujula, Georgi, and Glashow [17] and a relativistic quark-diquark potential model [18], respectively. Fleck and Richard,

using a variety of models, also predicted a mass value of $\sim$ 3600 [19], while Karliner et al. found $M_{\Xi_{cc}} = 3627 \pm 12$ MeV [20].

The new measurement of the LHCb Collaboration has stimulated much theoretical activity of the nonleptonic decays of doubly heavy baryons. The recent review can be found in Reference [21,22].

2. Light Baryons in SU(3)

In this section, let us recall the basic features of the $SU(3)$-classification of light baryons. Baryons are classified into multiplets according to decomposition of reducible product of the fundamental quark representations:

$$3 \otimes 3 \otimes 3 = 10 \oplus 8 \oplus 8' \oplus 1. \tag{1}$$

The octet representation **8** is written as (see Reference [23]):

$$B^i_j = \frac{1}{2}\left(T^i q_j - \frac{1}{3}\delta^i_j T^k q_k\right), \tag{2}$$

where a vector T^i belonging to the representation $\bar{\mathbf{3}}$ can be written as

$$T^i = \frac{1}{\sqrt{2}}\varepsilon^{ijk}(q_j q_k - q_k q_j), \quad \text{with quark triplet} \quad q = \begin{pmatrix} q_1 \\ q_2 \\ q_3 \end{pmatrix} = \begin{pmatrix} u \\ d \\ s \end{pmatrix}. \tag{3}$$

The matrix form of the octet representation looks like

$$B^i_j = \begin{pmatrix} \frac{1}{\sqrt{6}}\Lambda^0 + \frac{1}{\sqrt{2}}\Sigma^0 & \Sigma^+ & p \\ \Sigma^- & \frac{1}{\sqrt{6}}\Lambda^0 - \frac{1}{\sqrt{2}}\Sigma^0 & n \\ \Xi^- & \Xi^0 & -\frac{2}{\sqrt{6}}\Lambda^0 \end{pmatrix}. \tag{4}$$

The quark content of baryons are shown in Table 3.

Table 3. Quark content of the baryon octet.

$p \to \frac{1}{\sqrt{2}}[u,d]u$	$n \to \frac{1}{\sqrt{2}}[u,d]d$	
$\Sigma^+ \to \frac{1}{\sqrt{2}}[s,u]u$	$\Sigma^0 \to \frac{1}{2}([d,s]u + [u,s]d)$	$\Sigma^- \to \frac{1}{\sqrt{2}}[d,s]d$
$\Lambda^0 \to \frac{1}{\sqrt{12}}(-2[u,d]s + [d,s]u + [s,u]d)$	$\Xi^- \to \frac{1}{\sqrt{2}}[d,s]s$	$\Xi^0 \to \frac{1}{\sqrt{2}}[s,u]s$

Up to now, we discussed only the flavor structure of quark fields. Generally speaking, they also depend on color, spin, and space coordinates. Therefore, one has to construct the relativistic three quark currents with quantum numbers corresponding to certain member of the baryon octet. One can start from construction of qqq–currents, which are symmetric under permutation of all quarks in the case of exact $SU_F(3)$-symmetry. This program has been realized in Reference [24]. The starting point is the relativistic three-quark current with quantum numbers of a baryon octet $J^P = \frac{1}{2}^+$. The general form of this current can be written as

$$B^k_j \to R^{k;\,j_1,j_2,j_3}_j \, q^{a_1}_{j_1} q^{a_2}_{j_2} q^{a_3}_{j_3} \varepsilon_{a_1,a_2,a_3}, \tag{5}$$

where $j = (\alpha, m)$; a_i, α_i, m_i are the color, spinor, and flavor indices. By using the Fierz transformations for both Dirac matrices and $SU(3)$-matrices, one finds that there exist two independent currents for a baryon octet with quantum numbers $J^P = \frac{1}{2}^+$. They may be written in the form:

$$J^{km} = \varepsilon^{km_2m_1}\delta^{mm_3}\,\Gamma_1\,q^{a_1}_{m_1}\,(q^{a_2}_{m_2}C\Gamma_2 q^{a_3}_{m_3})\varepsilon_{a_1a_2a_3}, \tag{6}$$

where $\Gamma_1 \otimes \Gamma_2 = \gamma_\mu\gamma_5 \otimes \gamma^\mu$ (vector current) or $\sigma_{\mu\nu}\gamma_5 \otimes \sigma^{\mu\nu}$ (tensor current). $C = \gamma^0\gamma^2$ is the usual charge conjugation matrix:

$$\begin{aligned} C^T &= -C, \quad C^{-1} = C, \quad C^\dagger = C. \\ C\Gamma^T C^{-1} &= \begin{cases} +\Gamma & S, P, A \\ -\Gamma & V, T. \end{cases} \end{aligned}$$

One can check that the diquark with identical flavors exists for $\Gamma_2 = \gamma^\mu$ and $\sigma^{\mu\nu}$ only:

$$\begin{aligned} (u^{a_2}C\Gamma_2 u^{a_3})\varepsilon_{a_1a_2a_3} &= -(u^{a_3}\,(C\Gamma_2)^T\,u^{a_2})\varepsilon_{a_1a_2a_3} \\ &= -(u^{a_3}C\underbrace{C^{-1}\Gamma_2^T C^T}_{+\Gamma_2}u^{a_2})\varepsilon_{a_1a_2a_3} = +(u^{a_2}C\Gamma_2 u^{a_3})\varepsilon_{a_1a_2a_3}. \end{aligned}$$

Finally, the isotopic components for three-quark currents are written as in Table 4. The obtained expressions are coincided with those from Reference [25,26].

Table 4. Three-quark currents of the baryon octet (tensor Levi-Civita $\varepsilon_{a_1a_2a_3}$ skipped).

$p \to \Gamma_1 d_{a_1}(u_{a_2}C\Gamma_2 u_{a_3})$	$n \to \Gamma_1 u_{a_1}(d_{a_2}C\Gamma_2 d_{a_3})$	
$\Sigma^+ \to \Gamma_1 s_{a_1}(u_{a_2}C\Gamma_2 u_{a_3})$	$\Sigma^0 \to \sqrt{2}\,\Gamma_1 s_{a_1}(u_{a_2}C\Gamma_2 d_{a_3})$	$\Sigma^- \to \Gamma_1 s_{a_1}(d_{a_2}C\Gamma_2 d_{a_3})$
$\Lambda^0 \to \sqrt{\frac{2}{3}}\,\{\Gamma_1 u_{a_1}(d_{a_2}C\Gamma_2 s_{a_3}) - \Gamma_1 d_{a_1}(u_{a_2}C\Gamma_2 s_{a_3})\}$	$\Xi^- \to \Gamma_1 d_{a_1}(s_{a_2}C\Gamma_2 s_{a_3})$	$\Xi^0 \to \Gamma_1 u_{a_1}(s_{a_2}C\Gamma_2 s_{a_3})$

2.1. Fierz Transformations for Dirac Matrices

The basis of sixteen 4×4 Dirac matrices is shown in Table 5.

Table 5. Basis of Dirac matrices.

Scalar	S	I	1
Vector	V	γ^μ	4
Tensor	T	$\sigma^{\mu\nu} = \frac{i}{2}[\gamma^\mu, \gamma^\nu] \quad (\mu < \nu)$	6
Pseudoscalar	P	$\gamma_5 = i\gamma^0\gamma^1\gamma^2\gamma^3$	1
Axial	A	$i\gamma^\mu\gamma_5$	4
			16 total

The matrices from the basis satisfy to the normalization condition given by Equation (7) in general form and conditions given by Equation (8) for each matrix from the basis.

$$\boxed{\mathrm{tr}(\Gamma^C\Gamma^D) = 4\,\delta_{CD} \quad \text{where} \quad (C, D = S, V, T, P, A),} \tag{7}$$

$$\begin{array}{lcll} \mathrm{tr}(I_4 I_4) & = & 4, & \mathrm{tr}(\gamma^\mu\gamma^\nu) = 4\,g^{\mu\nu}\,, \\ \mathrm{tr}(\gamma_5\gamma_5) & = & 4, & \mathrm{tr}(i\gamma_5\gamma^\mu\cdot i\gamma_5\gamma^\nu) = 4\,g^{\mu\nu}\,, \\ \mathrm{tr}(\sigma^{\mu\nu}\sigma^{\alpha\beta}) & = & 4\,(g^{\mu\alpha}g^{\nu\beta} - g^{\mu\beta}g^{\nu\alpha})\,. & \end{array} \tag{8}$$

Any product of Dirac matrices can be decomposed into 16 independent matrices:

$$\Gamma = \sum_{D=S,V,T,P,A} C^D\Gamma^D, \quad \text{where} \quad 4\,C^D = \mathrm{tr}(\Gamma\Gamma^D). \tag{9}$$

One can derive from Equation (9) the useful property of the Dirac matrices called the *Fierz transformation*. One has

$$4\,\Gamma_{\alpha_1\alpha_2} = \sum_D \mathrm{tr}(\Gamma\Gamma^D)\Gamma^D_{\alpha_1\alpha_2} = \Gamma_{\alpha_4\alpha_3}\sum_D \Gamma^D_{\alpha_3\alpha_4}\Gamma^D_{\alpha_1\alpha_2} = 4\,\Gamma_{\alpha_1\alpha_2}. \tag{10}$$

The last equality holds if and only if the following property is valid:

$$\sum_{D=S,V,T,P,A} \Gamma^D_{\alpha_1\alpha_2}\Gamma^D_{\alpha_3\alpha_4} = 4\,\delta_{\alpha_1\alpha_4}\delta_{\alpha_3\alpha_2}. \tag{11}$$

By using following, Equation (11), one can arrive at the Fierz transformation

$$\begin{array}{rcl} 4\,\Gamma^{(1)}_{\alpha_1\alpha_2}\Gamma^{(2)}_{\alpha_3\alpha_4} & = & 4\,\delta_{\beta_2\alpha_2}\delta_{\beta_4\alpha_4}\,\Gamma^{(1)}_{\alpha_1\beta_2}\Gamma^{(2)}_{\alpha_3\beta_4} = \sum_D \Gamma^D_{\beta_2\alpha_4}\Gamma^D_{\beta_4\alpha_2}\,\Gamma^{(1)}_{\alpha_1\beta_2}\Gamma^{(2)}_{\alpha_3\beta_4} \\ & = & \sum_D (\Gamma^{(1)}\Gamma^D)_{\alpha_1\alpha_4}(\Gamma^{(2)}\Gamma^D)_{\alpha_3\alpha_2}. \end{array} \tag{12}$$

Then, we introduce the short notation.

$$\Gamma^{(1)}_{\alpha_1\alpha_2}\Gamma^{(2)}_{\alpha_3\alpha_4} = \widetilde{\Gamma^{(1)}}\otimes\widetilde{\Gamma^{(2)}}, \quad \text{and} \quad \Gamma^{(1)}_{\alpha_1\alpha_4}\Gamma^{(2)}_{\alpha_3\alpha_2} = \Gamma^{(1)}\otimes\Gamma^{(2)}. \tag{13}$$

There are a plenty of useful identities which relate the product of two Dirac matrices with tilde to product of two Dirac matrices without tilde. Here, are some of them:

$$\begin{array}{rcl} 4\,\widetilde{\gamma^\mu}\otimes\widetilde{\gamma_\mu} & = & +4\,I\otimes I - 2\,\gamma^\mu\otimes\gamma_\mu - 2\,\gamma^\mu\gamma_5\otimes\gamma_\mu\gamma_5 - 4\,\gamma_5\otimes\gamma_5 \\ 4\,\widetilde{\gamma^\mu\gamma_5}\otimes\widetilde{\gamma_\mu\gamma_5} & = & -4\,I\otimes I - 2\,\gamma^\mu\otimes\gamma_\mu - 2\gamma^\mu\gamma_5\otimes\gamma_\mu\gamma_5 + 4\,\gamma_5\otimes\gamma_5 \\ 4\,\widetilde{\gamma^\mu}\otimes\widetilde{\gamma_\mu\gamma_5} & = & -4\,I\otimes\gamma_5 + 4\,\gamma_5\otimes I - 2\gamma^\mu\otimes\gamma_\mu\gamma_5 - 2\,\gamma^\mu\gamma_5\otimes\gamma_\mu \\ 4\,\widetilde{\gamma^\mu\gamma_5}\otimes\widetilde{\gamma_\mu} & = & +4\,I\otimes\gamma_5 - 4\,\gamma_5\otimes I - 2\gamma^\mu\otimes\gamma_\mu\gamma_5 - 2\,\gamma^\mu\gamma_5\otimes\gamma_\mu \\ 4\,\widetilde{I}\otimes\widetilde{\gamma_5} & = & +I\otimes\gamma_5 + \gamma_5\otimes I - \gamma^\mu\otimes\gamma_\mu\gamma_5 + \gamma^\mu\gamma_5\otimes\gamma_\mu + \frac{1}{2}\,\sigma^{\mu\nu}\gamma_5\otimes\sigma_{\mu\nu} \\ 4\,\widetilde{\gamma_5}\otimes\widetilde{I} & = & +I\otimes\gamma_5 + \gamma_5\otimes I + \gamma^\mu\otimes\gamma_\mu\gamma_5 - \gamma^\mu\gamma_5\otimes\gamma_\mu + \frac{1}{2}\,\sigma^{\mu\nu}\gamma_5\otimes\sigma_{\mu\nu} \\ 4\,\widetilde{\sigma_{\mu\nu}\gamma_5}\otimes\widetilde{\sigma^{\mu\nu}} & = & +12\,I\otimes\gamma_5 + 12\,\gamma_5\otimes I - 2\,\sigma^{\mu\nu}\gamma_5\otimes\sigma_{\mu\nu}. \end{array}$$

We will use the above identities to simplify the string of Dirac matrices involving two weak matrices with Left/Right chirality $O^\mu_{L/R} = \gamma^\mu(I\mp\gamma_5)$. One can prove that

$$\widetilde{O_{L/R}}\otimes\widetilde{O_{L/R}} = -\,O_{L/R}\otimes O_{L/R}, \qquad \widetilde{O_{L/R}}\otimes\widetilde{O_{R/L}} = 2\,(I\pm\gamma_5)\otimes(I\mp\gamma_5). \tag{14}$$

By using these properties of the weak matrices, one can get the following simplifications:

$$\mathrm{tr}(\Gamma_1 O_{L/R}\Gamma_2 O_{L/R}) = -\,\mathrm{tr}(\Gamma_1 O_{L/R})\cdot\mathrm{tr}(\Gamma_2 O_{L/R}), \tag{15}$$

$$\Big(\Gamma_1 O_R\Gamma_2 O_L\Gamma_3\Big)^{\alpha\beta} = 2\,\Big(\Gamma_1(I-\gamma_5)\Gamma_3\Big)^{\alpha\beta}\cdot\mathrm{tr}\Big[\Gamma_2(I+\gamma_5)\Big]. \tag{16}$$

2.2. SU(n)-Matrices

Here, let us recall some properties of the unitary matrices from the $SU(n)$-group. For $SU(n)$-group, there are $m = n^2 - 1$ generators $t^a = \frac{1}{2}\lambda^a$, where λ^a are the Gell–Mann traceless $n \times n$ matrices ($a = 1, \ldots, m = n^2 - 1$). They satisfy the following relations:

$$\boxed{[\lambda^a, \lambda^b] = 2if^{abc}\lambda^c, \qquad \mathrm{tr}(\lambda^a\lambda^b) = 2\delta^{ab}, \quad (a, b = 1, \ldots, m).} \tag{17}$$

For completeness, one has to add the unit matrix $\lambda^0 = \sqrt{\frac{2}{n}}\, I_n$. Then, any $n \times n$ matrix can be decomposed into basis matrices:

$$M = \sum_{a=0}^{m} M^a\lambda^a, \qquad M^a = \frac{1}{2}\mathrm{tr}(\lambda^a M). \tag{18}$$

From Equation (18), it is easy to derive the completeness condition:

$$\sum_{a=0}^{m} \lambda^a_{m_1m_2}\lambda^a_{m_3m_4} = 2\,\delta_{m_1m_4}\delta_{m_3m_2}. \tag{19}$$

Some corollaries follow from Equation (19):

$$\boxed{\begin{array}{l} \sum\limits_{a=1}^{m} \lambda^a_{m_1m_2}\lambda^a_{m_3m_4} = 2\,\delta_{m_1m_4}\delta_{m_3m_2} - \dfrac{2}{n}\delta_{m_1m_2}\delta_{m_3m_4} \\ \sum\limits_{a=1}^{m} \lambda^a_{m_1m_2}\lambda^a_{m_3m_4} = \dfrac{2(n^2-1)}{n^2}\,\delta_{m_1m_4}\delta_{m_3m_2} - \dfrac{1}{n}\sum\limits_{a=1}^{m} \lambda^a_{m_1m_4}\lambda^a_{m_3m_2}. \end{array}} \tag{20}$$

They allow to simplify the calculation of traces:

$$\begin{array}{lcl} \sum\limits_{a=1}^{m} \mathrm{tr}\,(\lambda^a M_1\lambda^a M_2) & = & -\frac{2}{n}\mathrm{tr}\,(M_1M_2) + 2\,\mathrm{tr}\,(M_1)\,\mathrm{tr}\,(M_2) \\ \sum\limits_{a=1}^{m} \mathrm{tr}\,(\lambda^a M_1)\,\mathrm{tr}\,(\lambda^a M_2) & = & 2\,\mathrm{tr}\,(M_1M_2) - \frac{2}{n}\mathrm{tr}\,(M_1)\,\mathrm{tr}\,(M_2)\,. \end{array} \tag{21}$$

3. Charmed Baryons

The existence of a fourth quark had been discussed by a number of authors around 1964, for instance, by James Bjorken and Sheldon Glashow [4]. The addition of the charmed quark to the (uds) triplet extends the $SU(3)$ to $SU(4)$. The irreducible representations are formed according to decomposition

$$4 \otimes 4 \otimes 4 = 20_S \oplus 20_M \oplus 20'_M \oplus 4_A.$$

But, in that time, there was little evidence for existence of the charmed quark and related hadrons. Its prediction is usually credited to Glashow–Iliopoulos–Maiani [5] for the so-called GIM mechanism, which forbids the flavor-changing neutral currents in the tree diagrams.

GIM Mechanism

The attempt to construct the weak interactions with three (uds) quarks led to existence of the flavor-changing neutral current (FCNC) at tree level. The left weak duplet is written as

$$Q^u_L = \begin{pmatrix} u \\ d\cos\theta_C + s\sin\theta_C \end{pmatrix}_L, \tag{22}$$

where θ_C is the Cabbibo angle. It gives the following contribution to the weak Lagrangian

$$\begin{aligned}\bar{Q}^u_L\gamma^\mu\tfrac{\tau^3}{2}Q^u_L &= \tfrac{1}{2}\left(\bar{u}_L\gamma^\mu u_L-\cos^2\theta_C\bar{d}_L\gamma^\mu d_L-\sin^2\theta_C\bar{s}_L\gamma^\mu s_L\right.\\ &\left.-\sin\theta_C\cos\theta_C[\bar{d}_L\gamma^\mu s_L+\bar{s}_L\gamma^\mu d_L]\right).\end{aligned} \tag{23}$$

The charm quark allows one to construct an extra duplet:

$$Q^c_L=\begin{pmatrix} c \\ -d\sin\theta_C+s\cos\theta_C\end{pmatrix}_L. \tag{24}$$

It will give the additional contribution the the weak Lagrangian, where the FCNC contribute with the opposite sign:

$$\begin{aligned}\bar{Q}^c_L\gamma^\mu\frac{\tau^3}{2}Q^c_L &= \frac{1}{2}\left(\bar{c}_L\gamma^\mu c_L-\sin^2\theta_C\bar{d}_L\gamma^\mu d_L-\cos^2\theta_C\bar{s}_L\gamma^\mu s_L\right.\\ &\left.+\sin\theta_C\cos\theta_C(\bar{d}_L\gamma^\mu s_L+\bar{s}_L\gamma^\mu d_L)\right).\end{aligned}$$

As the result, the FCNC vanish from the weak Lagrangian and occur only at the level of loop diagrams:

$$\bar{Q}^u_L\gamma^\mu\frac{\tau^3}{2}Q^u_L+Q^c_L\gamma^\mu\frac{\tau^3}{2}Q^c_L=\tfrac{1}{2}\left(\bar{u}_L\gamma^\mu u_L+\bar{c}_L\gamma^\mu c_L-\bar{d}_L\gamma^\mu d_L-\bar{s}_L\gamma^\mu s_L\right). \tag{25}$$

For instance, the weak decay $K^0_L\to\mu^+\mu^-$ goes via sum of one-loop diagrams with u-quark and c-quark, as shown in Figure 1.

The matrix element is proportional to

$$M(K\to\mu^+\mu^-)\propto\frac{g_2^4\sin\theta_c\cos\theta_C}{M_W^2}\frac{m_c^2-m_u^2}{M_W^2}. \tag{26}$$

The experimental data can be reproduced if the value of the charm quark mass is of order $\longrightarrow$ $m_c\approx 1.5$ GeV. It was the first solid confirmation of the charm in particle physics.

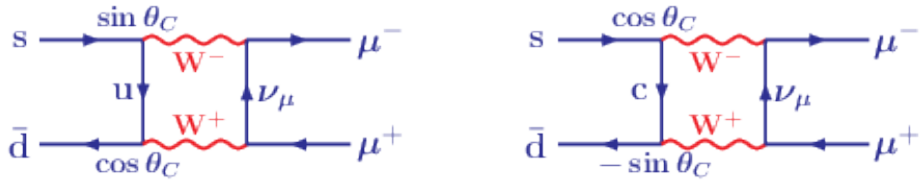

Figure 1. Diagrams describing the decay $K^0_L\to\mu^+\mu^-$. The left diagram describes the exchange by u-quark whereas the right by c-quark.

4. Nonleptonic Two-Body Weak Decays of Baryons

Ground states of baryons with $J^P=\frac{1}{2}^+$ can decay only weakly via the internal W-exchange. Two-body decays of baryons have five different quark topologies shown in Figure 2.

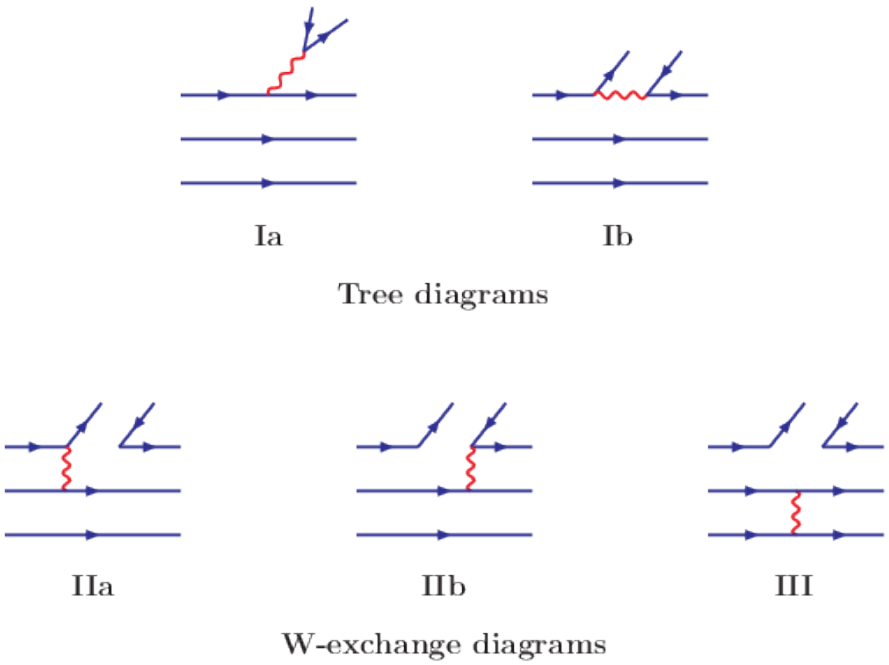

Figure 2. Quark diagrams with five different topologies. The set of diagrams divides in two groups: (1) The reducible tree-diagrams called external (Ia) and internal W-emission (IIb) diagrams. (2) The irreducible W-exchange diagrams with the labeling introduced in [7,16]. In [27] the W–exchange diagrams are denoted as the Exchange (IIa), color-commensurate (IIb) and Bow tie (III) diagram.

The weak interactions of quarks at energy significantly less than the W-mass, the scale of charm quark mass in the given decays, are described in the framework of an effective low-energy theory. The formal framework is using the Wilson operator product expansion (OPE). As an example, let us consider the tree-level W–exchange amplitude for $c \to su\bar{d}$ transition. One has

$$\begin{aligned} A &= -\frac{g_2^2}{8} V_{cs}^* V_{ud} \; (\bar{s} O^\mu c) \left(\frac{-g_{\mu\nu}}{M_W^2 - k^2} \right) (\bar{u} O^\nu d) \\ &= -\frac{g_2^2}{8\, M_W^2} V_{cs}^* V_{ud} \; (\bar{s} O^\mu c) \, (\bar{u} O_\mu d) + \mathcal{O}\left(\frac{k^2}{M_W^2} \right), \end{aligned} \tag{27}$$

where $O^\mu = \gamma^\mu (1 - \gamma_5)$ is the weak Dirac matrix with left chirality, V_{cs} and V_{ud} are the CKM-matrix elements, and g_2 is the coupling of gauge group. Since the momentum transfer is less than the W-mass, i.e., $|k| << M_W$, the terms of order $\mathcal{O}(k^2/M_W^2)$ may be neglected. It is easy to see that the leading term of the expansion can be obtained from an effective Hamiltonian

$$\mathcal{H}_{\text{eff}}^{\text{tree}} = \frac{G_F}{\sqrt{2}} V_{cs}^* V_{ud} \, (\bar{s}_a O^\mu c_a)(\bar{u}_b O_\mu d_b), \qquad \frac{G_F}{\sqrt{2}} = \frac{g_2^2}{8\, M_W^2}. \tag{28}$$

Then, one needs to take into account the one-loop QCD corrections both in full theory and in the theory with effective Hamiltonian. The corresponding tree and one-loop diagrams in full and effective theory are shown in Figure 3.

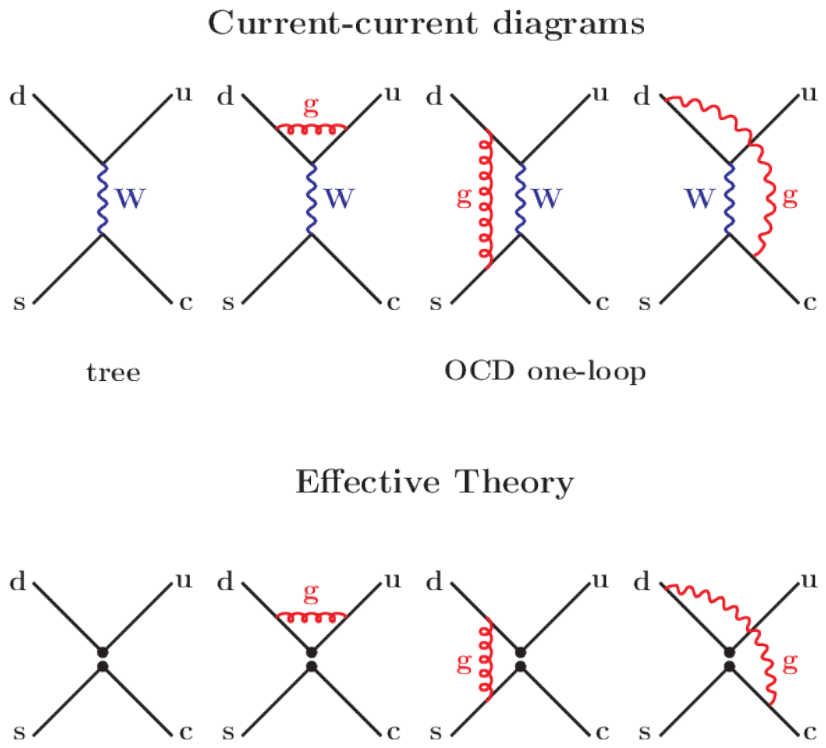

Figure 3. Tree and one-loop diagrams in full and effective theory. In the full theory the tree diagram is described by exchange of the W-boson, whereas in the effective theory the tree diagram is generated by four-quark operator from an effective Hamiltonian. In both theories the next-to-leading corrections are described by gluon (g) exchanges between color quarks.

Including QCD corrections, the effective Hamiltonian is generalized to

$$\begin{array}{rcl} \mathcal{H}_{\rm eff} & = & \frac{G_F}{\sqrt{2}} V_{cs}^* V_{ud} \; (C_1(\mu) Q_1 + C_2(\mu) Q_2)\,, \\ Q_1 & \equiv & (\bar{s}_a O^\mu c_b)(\bar{u}_b O_\mu d_a), \qquad Q_2 \equiv (\bar{s}_a O^\mu c_a)(\bar{u}_b O_\mu d_b), \end{array} \tag{29}$$

where the Wilson coefficients $C_i(\mu)$ are determined from the matching full and effective theories. The leading order in the strong QCD coupling α_S looks as follows:

$$C_1 = -3\frac{\alpha_S}{4\pi} \ln \frac{M_W^2}{\mu^2}, \qquad C_2 = 1 + \frac{\alpha_S}{4\pi} \ln \frac{M_W^2}{\mu^2}. \tag{30}$$

Obviously, this expansion will be reliable if the scale μ is of order of W-mass, i.e., $\mu \approx M_W$). In this case, the value of α_S is small due to asymptotic freedom, and the value of the logarithm is small, as well. Then, the Wilson coefficients are evaluated from μ_W down to the low-energy scale $\mu \propto m_c$. The last step is to calculate the hadronic matrix elements of the operators $\langle Q_i(\mu) \rangle$ that requires the nonperturbative methods.

5. Covariant Constituent Quark Model

The Covariant Constituent Quark Model (CCQM) is based on a phenomenological, nonlocal, relativistic Lagrangian describing the coupling of a hadron H to its constituents:

$$\mathcal{L}_{\rm int} = g_H \cdot H(x) \cdot J_H(x), \tag{31}$$

where $J_H(x)$ is the quark current corresponding to a hadron H. For mesons, baryons, and tetraquarks, the corresponding quark currents may be written as

$$\begin{array}{rcl} J_M(x) & = & \int dx_1 \int dx_2\, F_M(x;x_1,x_2)\cdot \bar{q}^{\,a}_{f_1}(x_1)\,\Gamma_M\, q^{a}_{f_2}(x_2), \\ J_B(x) & = & \int dx_1 \int dx_2 \int dx_3\, F_B(x;x_1,x_2,x_3)\times \Gamma_1\, q^{a_1}_{f_1}(x_1)\left(\varepsilon^{a_1a_2a_3} q^{T\,a_2}_{f_2}(x_2) C\,\Gamma_2\, q^{a_3}_{f_3}(x_3)\right) \\ J_T(x) & = & \int dx_1 \ldots \int dx_4\, F_T(x;x_1,\ldots,x_4) \\ & & \times \left(\varepsilon^{a_1a_2c} q^{T\,a_1}_{f_1}(x_1)\, C\Gamma_1\, q^{a_2}_{f_2}(x_2)\right)\cdot\left(\varepsilon^{a_3a_4c}\bar{q}^{T\,a_3}_{f_3}(x_3)\,\Gamma_2 C\,\bar{q}^{a_4}_{f_4}(x_4)\right). \end{array} \tag{32}$$

where a_i and f_i are color and flavor indices. The vertex functions F_H should satisfy to translational invariance

$$F_H(x+a;x_1+a,\ldots,x_n+a) = F_H(x;x_1,\ldots,x_n)\,, \qquad \forall a\,. \tag{33}$$

The simple and obvious choice is written down as

$$\begin{array}{rcl} F_H(x,x_1,\ldots,x_n) & = & \delta^{(4)}\Big(x-\sum\limits_{i=1}^{n} w_i x_i\Big)\,\Phi_H\Big(\sum\limits_{i<j}(x_i-x_j)^2\Big), \\ \Phi_H\big(\sum\limits_{i<j}(x_i-x_j)^2\big) & = & \prod\limits_{i=1}^{n-1}\int\frac{d^4q_i}{(2\pi)^4}\, e^{-iq_1(x_1-x_n)-iq_2(x_2-x_n)-\ldots-iq_{n-1}(x_{n-1}-x_n)}\widetilde{\Phi}_H\left(-\tfrac{1}{2}\sum\limits_{i\le j} q_i q_j\right), \\ \widetilde{\Phi}_H(-\Omega) & = & \exp\{\Omega/\Lambda_H^2\}, \end{array} \tag{34}$$

where $w_i = m_i/\sum\limits_j m_j$ so that $\sum\limits_{i=1}^{n} w_i = 1$, and Λ_H is an adjustable size parameter. The quark propagators are chosen in the local Dirac form

$$S_i(x_1-x_2) = \int \frac{d^4k}{(2\pi)^4 i}\frac{e^{-ik(x_1-x_2)}}{m_i - \not{k}}. \tag{35}$$

The quark confinement is realized by implementation of the so-called infrared confinement. We discuss how it works in the next sections.

5.1. Heavy Quark Limit in $B - D(D^*)$ Transition

It is instructive to explore the heavy quark limit (HQL) in the heavy-to-heavy transition $B \to D(D^*)$. The diagram describing the semileptonic decay $B \to D(D^*) + \ell\bar{\nu}_\ell$ is shown in Figure 4.

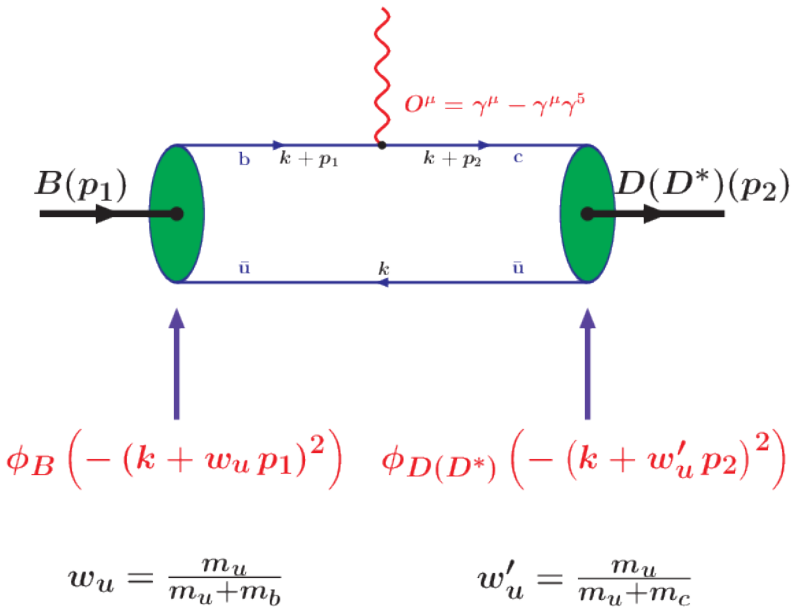

Figure 4. Diagrams describing the semileptonic decay $B \to D(D^*) + \ell\bar{\nu}_\ell$.

In the HQL, one takes the limit $m_B = m_b + E,\ \ m_b \to \infty$ and $m_D = m_{D^*} = m_c + E,\ \ m_c \to \infty$ in the expressions for the coupling constants and form factors. In this limit, the heavy quark propagators are reduced to the static form:

$$\begin{aligned} S_b(k+p_1) &= \frac{1}{m_b - \not{k} - \not{p}_1} \to \frac{1 + \not{v}_1}{-2kv_1 - 2E} + O\left(\frac{1}{m_b}\right), \\ S_c(k+p_2) &= \frac{1}{m_c - \not{k} - \not{p}_2} \to \frac{1 + \not{v}_2}{-2kv_2 - 2E} + O\left(\frac{1}{m_c}\right), \end{aligned} \tag{36}$$

where p_i and $v_i = p_i/m_i$ $(i = 1, 2)$ are the momenta and the four-velocities of the initial and final states. Moreover, we have to keep the size parameters of heavy hadrons equal to each other in order to provide the correct normalization of the Isgur-Wise function at zero recoil. By using technique developed in our previous papers [28,29], one can arrive at the following expressions for the semileptonic heavy-to-heavy transitions:

$$T^\mu_{\rm HQL} = \xi(w) \cdot \tfrac{1}{4}{\rm tr}\Big(O^\mu(1 + \not{v}_1)\gamma^5 \cdot \gamma^5(1 + \not{v}_2)\Big) = \xi(w) \cdot (v_1^\mu + v_2^\mu), \tag{37}$$

$$\begin{aligned} \epsilon^\dagger_{2\nu} T^{\mu\nu}_{\rm HQL} &= \xi(w) \cdot \tfrac{1}{4}{\rm tr}\Big(O^\mu(1 + \not{v}_1)\gamma^5 \cdot \not{\epsilon}^\dagger_2(1 + \not{v}_2)\Big) \\ &= \xi(w) \cdot \epsilon^\dagger_{2\nu}(-g^{\mu\nu}(1 + w) + v_1^\mu v_2^\nu + v_1^\nu v_2^\mu - i\,\varepsilon^{\mu\nu v_1 v_2}). \end{aligned} \tag{38}$$

Here, $w = v_1 v_2$, and the Isgur-Wise function is equal to

$$\xi(w) = \frac{J_3(E, w)}{J_3(E, 1)}, \qquad J_3(E, w) = \int_0^1 \frac{d\tau}{W} \int_0^\infty du\, \widetilde{\Phi}^2(z) \frac{m_u + \sqrt{u/W}}{m_u^2 + z}, \tag{39}$$

where $W = 1 + 2\tau(1-\tau)(w-1)$, $z = u - 2E\sqrt{u/W}$, and $\widetilde{\Phi}(z) = \exp(-z/\Lambda^2)$. By using the definition of the form factors given in Reference [28,29], one can easily obtain the expressions of the form factors in the HQL. One finds

$$\begin{array}{rcl} F_\pm(q^2) & = & \pm\frac{m_1 \pm m_2}{2\sqrt{m_1 m_2}}\,\xi(w), \\ A_0(q^2) & = & \frac{\sqrt{m_1 m_2}}{m_1 - m_2}(1+w)\xi(w), \quad A_+(q^2) = -A_-(q^2) = V(q^2) = \frac{m_1+m_2}{2\sqrt{m_1 m_2}}\,\xi(w), \end{array} \tag{40}$$

where $w = (m_1^2 + m_2^2 - q^2)/(2m_1 m_2)$. We use the physical masses of the heavy hadrons in the numerical calculations. For the size parameter, we adopt the average value $\Lambda = (\Lambda_B + \Lambda_D + \Lambda_{D^*})/3 = 1.70$ GeV. The parameter E characterizes the difference in mass between the heavy hadron and the corresponding heavy quark. We use its minimal value $E = m_D - m_c = 0.20$ GeV in order to avoid the complication with confinement. In Figure 5, we display the heavy-to-heavy transition form factors calculated in the HQL and compare them with the results of exact calculations [30]. One can see that the two results obtained with and without use of the HQL behave very similar to each other, which demonstrates the fidelity of HQET.

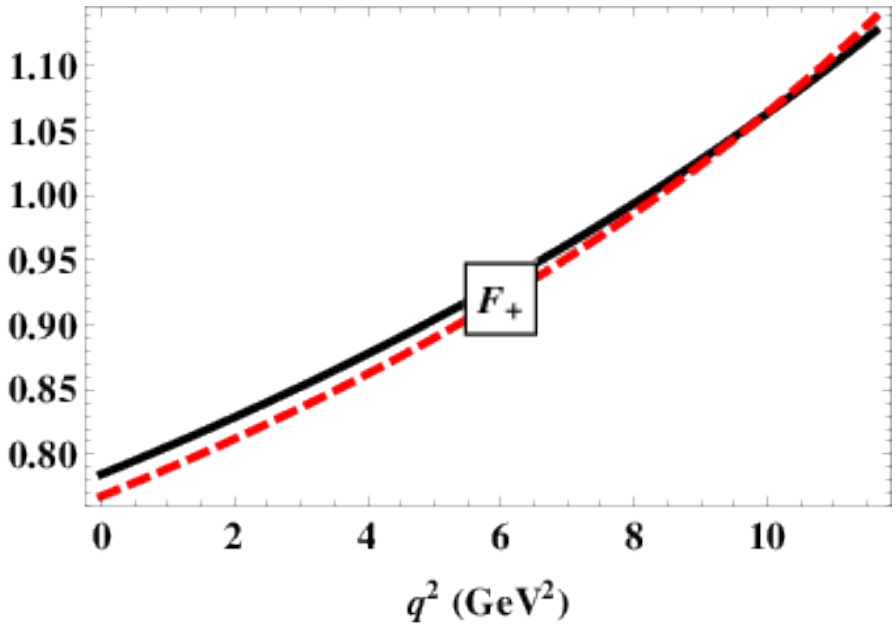

Figure 5. Comparison of the exact calculation of the form factor $F_+(q^2)$ (solid line) with those obtained in heavy quark limit (dashed line).

5.2. Infrared Confinement

We have shown in Reference [31] how the confinement of quarks can be effectively incorporated in the covariant quark model. In a first step, we introduced an additional scale integration in the space of Fock-Schwinger's α–parameters with an integration range from zero to infinity. In a second step, the scale integration was cut off at the upper limit which corresponds to the introduction of an infrared (IR) cutoff. In this manner, all possible thresholds present in the initial quark diagram were removed. The cutoff parameter was taken to be the same for all physical processes. Other model parameters, such as the constituent quark masses and size parameters, were determined from a fit to experimental data.

Let us describe the basic features of how IR confinement is implemented in our model. All physical matrix elements are described by Feynman diagrams written in terms of a convolution of

free quark propagators and the vertex functions. In computation of Feynman diagrams, we use, in the momentum space, the Fock-Schwinger representation of the quark propagator:

$$S(k) = \frac{m + \not{k}}{m^2 - k^2} = (m + \not{k}) \int\limits_0^\infty d\alpha \, e^{-\alpha\left(m^2 - k^2\right)}. \tag{41}$$

The general form of a resulting Feynman diagrams is

$$\Pi\left(p_1, \ldots, p_m\right) = \int\limits_0^\infty d^n\alpha \int \left(d^4k\right)^\ell \times \mathrm{Num} \times \exp\left\{-\sum_{i=1}^n \alpha_i \left(m_i^2 - \left(K_i + P_i\right)^2\right)\right\}, \tag{42}$$

where K_i represents a linear combination of loop momenta, P_i stands for a linear combination of external momenta, and Num refers to the numerator product of propagators and vertex functions. The integrand in Equation (42) has a Gaussian form with the exponential factor

$$kak + 2kr + R = k_i a_{ij} k_j + 2k_i r_i + R, \qquad (i, j = 1, \ldots, \ell),$$

where k_i is a 4-vector of the "i"-loop integration, a is a $\ell \times \ell$ matrix depending on the parameters α_i and size parameters Λ, r_i is a 4- vector composed from the external momenta p_i, and R is a quadratic form of the masses and external momenta. Tensor loop integrals are calculated with the help of the differential representation

$$k_i^\mu e^{2kr} = \frac{1}{2}\frac{\partial}{\partial r_{i\,\mu}} e^{2kr},$$

which, in general, may be written in the form

$$\int \left(d^4k\right)^\ell P\left(k\right) e^{kak + 2kr + R} = \int \left(d^4k\right)^\ell P\left(\frac{1}{2}\frac{\partial}{\partial r}\right) e^{kak + 2kr + R} = P\left(\frac{1}{2}\frac{\partial}{\partial r}\right) \int \left(d^4k\right)^\ell e^{kak + 2kr + R}, \tag{43}$$

where the polynomial operator means $P(k) = k_1^{\mu_1} \ldots k_m^{\mu_m}$. After doing the loop integration, the differential operators $\partial/\partial r_{i\,\mu}$ will give cause to outer momenta tensors. It may be done in effective way by using the identity

$$\int\limits_0^\infty d^n\alpha \, P\left(\frac{1}{2}\frac{\partial}{\partial r}\right) e^{-\frac{r^2}{a}} = \int\limits_0^\infty d^n\alpha \, e^{-\frac{r^2}{a}} P\left(\frac{1}{2}\frac{\partial}{\partial r} - \frac{r}{a}\right). \tag{44}$$

The calculation of the polynomial $P\left(\frac{1}{2}\frac{\partial}{\partial r} - \frac{r}{a}\right)$ can be automized by using the commutator $\left[\frac{\partial}{\partial r_i^\mu}, r_j^\nu\right] = \delta_{ij}\, g^{\mu\nu}$. We have written a FORM [32] program that achieves the necessary commutations of the differential operators in a very efficient way.

The last point which remains to be discussed is the infrared cut-off we impose on the integration over the Fock-Schwinger parameters. This integration is multidimensional with the limits from 0 to $+\infty$. In order to arrive to a single cut-off parameter, we first transform the integral over an infinite space into an integral over a simplex convoluted with only one-dimensional improper integral. For that purpose, we use the δ-function form of the identity

$$1 = \int\limits_0^\infty dt \, \delta\left(t - \sum_{i=1}^n \alpha_i\right), \qquad (\forall \alpha_i \geq 0), \tag{45}$$

from which follows

$$\Pi = \int\limits_0^\infty dt\, t^{n-1} \int\limits_0^1 d^n\alpha\, \delta\left(1 - \sum_{i=1}^n \alpha_i\right) \times W\left(t\alpha_1, \ldots, t\alpha_1\right), \tag{46}$$

where W represents the integrand of Schwinger parameters. The cut-off λ is then introduced in a natural way:

$$\int\limits_0^\infty dt\, t^{n-1} \ldots \to \int\limits_0^{1/\lambda^2} dt\, t^{n-1} \ldots . \tag{47}$$

Such a cut-off makes the integral to be an analytic function without any singularities. In this way, all potential thresholds in the quark loop diagrams are removed together with corresponding branch points [31]. Within the covariant quark model, the cut-off parameter is universal for all processes, and its value, as obtained from a fit to data, is

$$\lambda_{\rm cut-off} = 0.181\,{\rm GeV}.$$

The numerical evaluations have been done by a numerical program written in the fortran code.

As an example, let us consider a scalar one-loop two-point function:

$$\Pi_2(p^2) = \int \frac{d^4k_E}{\pi^2} \frac{e^{-s\,k_E^2}}{[m^2 + (k_E + \frac{1}{2}p_E)^2][m^2 + (k_E - \frac{1}{2}p_E)^2]},$$

where the numerator factor $e^{-s\,k_E^2}$ comes from the product of nonlocal vertex form factors of Gaussian form. k_E, p_E are Euclidean momenta ($p_E^2 = -\,p^2$). Doing the loop integration, one obtains

$$\Pi_2(p^2) = \int\limits_0^\infty dt \frac{t}{(s+t)^2} \int\limits_0^1 d\alpha\, \exp\Big\{ -\, t\,[m^2 - \alpha(1-\alpha)p^2] + \frac{st}{s+t}\Big(\alpha - \frac{1}{2}\Big)^2 p^2\Big\}. \tag{48}$$

The function $\Pi_2(p^2)$ has a branch point at $p^2 = 4m^2$, which occurs at $\alpha = 1/2$. By introducing a cut-off in the t–integration, one obtains

$$\Pi_2^c(p^2) = \int\limits_0^{1/\lambda^2} dt \frac{t}{(s+t)^2} \int\limits_0^1 d\alpha\, \exp\Big\{ -\, t\,[m^2 - \alpha(1-\alpha)p^2] + \frac{st}{s+t}\Big(\alpha - \frac{1}{2}\Big)^2 p^2\Big\}, \tag{49}$$

where the one-loop two-point function $\Pi_2^c(p^2)$ no longer has a branch point at $p^2 = 4m^2$. The confinement scenario also allows us to include all possible, both two-quark and multi-quark, resonance states in our calculations.

6. Some Nonleptonic Decays of Doubly Charmed Baryons

We will consider the decays that belong to the same topology class:

$$\begin{array}{lcll} \Xi_{cc}^{++} & \to & \Xi_c^+\,(\Xi_c'^+) + \pi^+(\rho^+) & \text{T-Ia and W-IIb} \\ \Omega_{cc}^{+} & \to & \Xi_c^+\,(\Xi_c'^+) + \bar{K}^0(K^{*0}) & \text{T-Ib and W-IIb.} \end{array} \tag{50}$$

Their quantum numbers and interpolating currents are shown in Table 6.

Table 6. Interpolating currents.

Baryon	J^P	Interpolating Current	Mass (MeV)
Ξ_{cc}^{++}	$\frac{1}{2}^+$	$\varepsilon_{abc}\,\gamma^\mu\gamma_5\,u^a(c^bC\gamma_\mu c^c)$	3620.6
Ω_{cc}^{+}	$\frac{1}{2}^+$	$\varepsilon_{abc}\,\gamma^\mu\gamma_5\,s^a(c^bC\gamma_\mu c^c)$	3710.0
$\Xi_c^{\prime+}$	$\frac{1}{2}^+$	$\varepsilon_{abc}\,\gamma^\mu\gamma_5\,c^a(u^bC\gamma_\mu s^c)$	2577.4
Ξ_c^{+}	$\frac{1}{2}^+$	$\varepsilon_{abc}\,c^a(u^bC\gamma_5 s^c)$	2467.9

The W–exchange contributions to the above decays fall into two classes:

1. The decays with a $\Xi_c^{\prime+}$-baryon containing a symmetric $\{us\}$ diquark described by the interpolating current $\varepsilon_{abc}\,(u^bC\gamma_\mu s^c)$. The W–exchange contribution is strongly suppressed due to the Körner-Pati-Woo (KPW) theorem [33,34], which states that the contraction of the flavor antisymmetric current-current operator with a flavor symmetric final state configuration is zero in the $SU(3)$ limit.
2. The decays with a Ξ_c^{+}-baryon containing a antisymmetric $[us]$ diquark described by the interpolating current $\varepsilon_{abc}\,(u^bC\gamma_5 s^c)$. In this case, the W–exchange contribution is not a priori suppressed.

In our approach, the tree and W–exchange contributions are described by the Feynman diagrams shown in Figure 6.

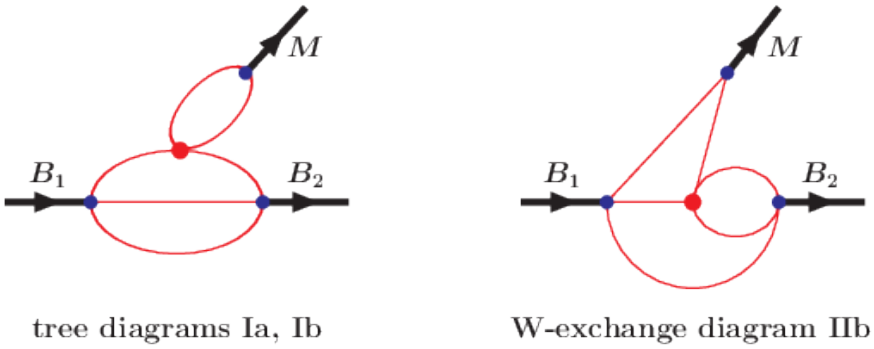

Figure 6. Diagrams describing the nonleptonic decay $B_1 \to B_2 + M$.

The matrix element is written down as

$$< B_2\,M|\mathcal{H}_{\rm eff}|B_1 >= \frac{G_F}{\sqrt{2}}V_{cs}V_{ud}^{\dagger}\,\bar{u}(p_2)\Big(12\,C_T\,M_T + 12\,(C_1-C_2)\,M_W\Big)u(p_1), \tag{51}$$

where the combinations of the Wilson coefficients are given by

$$C_T = \begin{cases} C_T = +(C_2+\xi C_1) & \text{charged meson} \\ C_T = -(C_1+\xi C_2) & \text{neutral meson.} \end{cases}$$

The factor of $\xi = 1/N_c$ is set to zero in the numerical calculations. The contribution from the tree diagram factorizes into two pieces:

$$M_T = M_T^{(1)} \cdot M_T^{(2)}, \tag{52}$$

where

$$
\begin{aligned}
M_T^{(1)} &= N_c\, g_M \int \frac{d^4k}{(2\pi)^4 i} \widetilde{\Phi}_M(-k^2)\, \mathrm{tr}\left(O_L S_d(k - w_d q) \Gamma_M S_{s(u)}(k + w_{s(u)} q) \right), \\
M_T^{(2)} &= g_{B_1} g_{B_2} \int \frac{d^4k_1}{(2\pi)^4 i} \int \frac{d^4k_2}{(2\pi)^4 i} \widetilde{\Phi}_{B_1}\Big(-\vec{\Omega}_1^2 \Big) \widetilde{\Phi}_{B_2}\Big(-\vec{\Omega}_2^2 \Big) \\
&\times \Gamma_1 S_c(k_2) \gamma^\mu S_c(k_1 - p_1) O_R S_{u(s)}(k_1 - p_2) \widetilde{\Gamma}_2 S_{s(u)}(k_1 - k_2) \gamma_\mu \gamma_5 .
\end{aligned}
$$

The $M_T^{(1)}$ is related to the leptonic decay constants:

$$
M_T^{(1)} = \begin{cases} -f_P \cdot q & \text{pseudoscalar meson} \\ +f_V m_V \cdot \epsilon_V & \text{vector meson.} \end{cases}
$$

The semileptonic and nonleptonic two-body decays of the doubly charmed baryons Ξ_{cc}^{++}, Ξ_{cc}^{+} and Ω_{cc}^{+} have been studied in Reference [35] by considering those nonleptonic decay channels in which the decay proceeds solely via the factorizing contributions.

The W–exchange contribution has no factorization and is written as genuine three-loop diagram:

$$
\begin{aligned}
M_W &= g_{B_1} g_{B_2} g_M \int \frac{d^4k_1}{(2\pi)^4 i} \int \frac{d^4k_2}{(2\pi)^4 i} \int \frac{d^4k_3}{(2\pi)^4 i} \widetilde{\Phi}_{B_1}\Big(-\vec{\Omega}_1^2 \Big) \widetilde{\Phi}_{B_2}\Big(-\vec{\Omega}_2^2 \Big) \widetilde{\Phi}_M(-P^2) \\
&\times 2\Gamma_1 S_c(k_1) \gamma^\mu S_c(k_2)(1 - \gamma_5) S_d(k_2 - k_1 + p_2) \Gamma_M S_{s(u)}(k_2 - k_1 + p_1) \gamma_\mu \gamma_5 \\
&\times \mathrm{tr}\Big(S_{u(s)}(k_3) \widetilde{\Gamma}_2 S_{s(u)}(k_3 - k_1 + p_2)(1 + \gamma_5) \Big).
\end{aligned}
$$

Here, $\Gamma_1 \otimes \widetilde{\Gamma}_2 = I \otimes \gamma_5$ for $B_2 = \Xi_c^+$, and $-\gamma_\nu \gamma_5 \otimes \gamma^\nu$ for $B_2 = \Xi_c^{\prime +}$. To verify the KPW theorem in the case of $B_2 = \Xi_c^{\prime +}$, we use the identity

$$
\mathrm{tr}\Big(S_u(k_3) \gamma_\nu S_s(k_3 - k_1 + p_2) \Big) = -\,\mathrm{tr}\Big(S_s(-k_3 + k_1 - p_2) \gamma_\nu S_u(-k_3) \Big). \tag{53}
$$

Then, by shifting $k_3 \to -k_3 + k_1 - p_2$, one gets the same expression with opposite sign and $u \leftrightarrow s$ interchange. Thus, if $m_u = m_s$, then $M_W \equiv 0$. It directly confirms the KPW–theorem.

7. Numerical Results

The transition amplitudes in terms of invariant amplitudes are written down as

$$
\begin{aligned}
< B_2\, P | \mathcal{H}_{\mathrm{eff}} | B_1 > &= \frac{G_F}{\sqrt{2}} V_{cs}^* V_{ud}\, \bar{u}(p_2)\, (A + \gamma_5\, B)\, u(p_1) \\
< B_2\, V | \mathcal{H}_{\mathrm{eff}} | B_1 > &= \frac{G_F}{\sqrt{2}} V_{cs}^* V_{ud} \\
&\times \bar{u}(p_2)\, \epsilon_{V\delta}^* \left(\gamma^\delta V_\gamma + p_1^\delta V_p + \gamma_5 \gamma^\delta V_{5\gamma} + \gamma_5 p_1^\delta\, V_{5p} \right) u(p_1)
\end{aligned}
$$

The invariant amplitudes can be expressed in terms of helicity amplitudes as

$$
\begin{aligned}
H^V_{\frac{1}{2}\, t} &= \sqrt{Q_+}\, A \qquad H^A_{\frac{1}{2}\, t} = \sqrt{Q_-}\, B \\
H^V_{\frac{1}{2}\, 0} &= +\sqrt{Q_-/q^2} \left(m_+\, V_\gamma + \tfrac{1}{2} Q_+\, V_p \right) \qquad H^V_{\frac{1}{2}\, 1} = -\sqrt{2Q_-}\, V_\gamma \\
H^A_{\frac{1}{2}\, 0} &= +\sqrt{Q_+/q^2} \left(m_-\, V_{5\gamma} + \tfrac{1}{2} Q_-\, V_{5p} \right) \qquad H^A_{\frac{1}{2}\, 1} = -\sqrt{2Q_+}\, V_{5\gamma}.
\end{aligned} \tag{54}
$$

Here, $m_\pm = m_1 \pm m_2$, $Q_\pm = m_\pm^2 - q^2$ and $|\mathbf{p_2}| = \lambda^{1/2}(m_1^2, m_2^2, q^2)/(2m_1)$. The parity relations have taken place: $H^V_{-\lambda_2,-\lambda_M} = +H^V_{\lambda_2,\lambda_M}, H^A_{-\lambda_2,-\lambda_M} = -H^A_{\lambda_2,\lambda_M}$. Finally, the decay widths are written as

$$\begin{aligned}
\Gamma\Big(B_1 \to B_2 + P(V)\Big) &= \frac{G_F^2}{32\pi}\,|V_{cs}^* V_{ud}|^2\,\frac{|\mathbf{p_2}|}{m_1^2}\,\mathcal{H}_{P(V)} \\
\mathcal{H}_P &= \left|H_{\frac{1}{2}\,t}\right|^2 + \left|H_{-\frac{1}{2}\,t}\right|^2, \\
\mathcal{H}_V &= \left|H_{\frac{1}{2}\,0}\right|^2 + \left|H_{-\frac{1}{2}\,0}\right|^2 + \left|H_{\frac{1}{2}\,1}\right|^2 + \left|H_{-\frac{1}{2}\,-1}\right|^2,
\end{aligned}$$

where $H = H^V - H^A$. All model parameters have been fixed in our previous studies, except for the size parameter Λ_{cc} of the doubly charmed baryons. As a first approximation, we equate the size parameter of doubly charmed baryons with that of singly charmed baryons, i.e., we take $\Lambda_{cc} = \Lambda_c = 0.8675$ GeV, where we adopt the value of Λ_c from Reference [36] obtained by fitting the magnetic moment of Λ_c to its experimental value.

Numerical results for the helicity amplitudes and decay widths are displayed in the Tables 7–10.

Our results highlight the importance of the KPW theorem for the nonleptonic decays when the final state involves a Ξ'^+ baryon containing a symmetric $\{su\}$ diquark. Tables 7–10 show that the relevant W–exchange contributions are nonzero but are strongly suppressed. Nonzero values result from $SU(3)$ breaking effects, which are accounted for in our approach. Take, for example, the decay $\Xi_{cc}^{++} \to \Xi_c^{'+} + \pi^+$. When compared to the tree contribution, the $SU(3)$ breaking effects amount to $\sim (2-4)\,\%$. While the consequences of the KPW theorem for the W–exchange contribution are also incorporated in the pole model approach of Reference [37] (see Figure 7), they are not included in the final-state interaction approach of Reference [38].

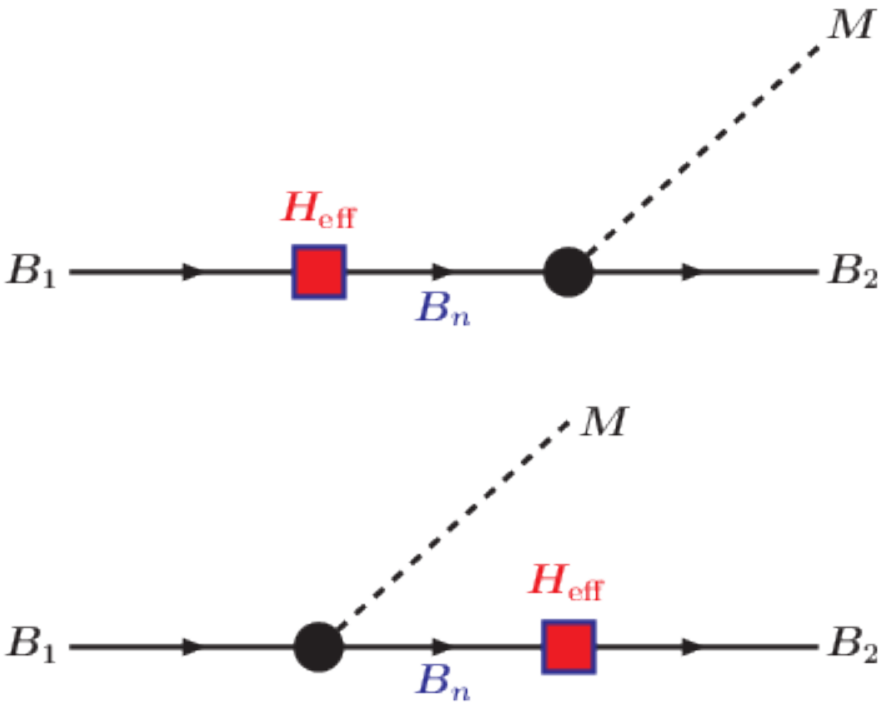

Figure 7. Schematic image of the pole model.

Table 7. Decays $\Omega_{cc}^{+} \to \Xi_c'^{+} + \bar{K}^0(\bar{K}^{*0})$.

Helicity	Tree Diagram	*W* Diagram	Total
$H^V_{\frac{1}{2}\,t}$	0.20	-0.01	0.19
$H^A_{\frac{1}{2}\,t}$	0.25	-0.01	0.24
$\Gamma(\Omega_{cc}^{+} \to \Xi_c'^{+} + \bar{K}^0) = 0.15 \cdot 10^{-13}\,\mathrm{GeV}$			
$H^V_{\frac{1}{2}\,0}$	-0.25	0.04×10^{-1}	-0.25
$H^A_{\frac{1}{2}\,0}$	-0.50	0.01	-0.49
$H^V_{\frac{1}{2}\,1}$	0.27	-0.01	0.26
$H^A_{\frac{1}{2}\,1}$	0.56	0.04×10^{-2}	0.56
$\Gamma(\Omega_{cc}^{+} \to \Xi_c'^{+} + \bar{K}^{*0}) = 0.74 \cdot 10^{-13}\,\mathrm{GeV}$			

Table 8. Decays $\Omega_{cc}^{+} \to \Xi_c^{+} + \bar{K}^0(\bar{K}^{*0})$.

Helicity	Tree Diagram	*W* Diagram	Total
$H^V_{\frac{1}{2}\,t}$	-0.35	1.06	0.71
$H^A_{\frac{1}{2}\,t}$	-0.10	0.31	0.21
$\Gamma(\Omega_{cc}^{+} \to \Xi_c^{+} + \bar{K}^0) = 0.95 \cdot 10^{-13}\,\mathrm{GeV}$			
$H^V_{\frac{1}{2}\,0}$	0.50	-0.69	-0.19
$H^A_{\frac{1}{2}\,0}$	0.18	-0.45	-0.27
$H^V_{\frac{1}{2}\,1}$	-0.11	-0.24	-0.35
$H^A_{\frac{1}{2}\,1}$	-0.18	0.66	0.48
$\Gamma(\Omega_{cc}^{+} \to \Xi_c^{+} + \bar{K}^{*0}) = 0.62 \cdot 10^{-13}\,\mathrm{GeV}$			

Table 9. Decays $\Xi_{cc}^{++} \to \Xi_c'^{+} + \pi^{+}(\rho^{+})$.

Helicity	Tree Diagram	*W* Diagram	Total
$H^V_{\frac{1}{2}\,t}$	-0.38	-0.01	-0.39
$H^A_{\frac{1}{2}\,t}$	-0.55	-0.02	-0.57
$\Gamma(\Xi_{cc}^{++} \to \Xi_c'^{+} + \pi^{+}) = 0.82 \cdot 10^{-13}\,\mathrm{GeV}$			
$H^V_{\frac{1}{2}\,0}$	0.60	0.04×10^{-1}	0.61
$H^A_{\frac{1}{2}\,0}$	1.20	0.01	1.21
$H^V_{\frac{1}{2}\,1}$	-0.49	-0.01	-0.50
$H^A_{\frac{1}{2}\,1}$	-1.27	0.01×10^{-1}	-1.27
$\Gamma(\Xi_{cc}^{++} \to \Xi_c'^{+} + \rho^{+}) = 4.27 \cdot 10^{-13}\,\mathrm{GeV}$			

Table 10. Decays $\Xi_{cc}^{++} \to \Xi_c^+ + \pi^+(\rho^+)$.

Helicity	Tree Diagram	*W* Diagram	Total
$H^V_{\frac{1}{2}\,t}$	−0.70	0.99	0.29
$H^A_{\frac{1}{2}\,t}$	−0.21	0.30	0.09
$\Gamma(\Xi_{cc}^{++} \to \Xi_c^+ + \pi^+) = 0.18 \cdot 10^{-13}\,\text{GeV}$			
$H^V_{\frac{1}{2}\,0}$	1.17	−0.70	0.47
$H^A_{\frac{1}{2}\,0}$	0.45	−0.44	0.003
$H^V_{\frac{1}{2}\,1}$	−0.20	−0.23	−0.43
$H^A_{\frac{1}{2}\,1}$	−0.41	0.62	0.21
$\Gamma(\Xi_{cc}^{++} \to \Xi_c^+ + \rho^+) = 0.63 \cdot 10^{-13}\,\text{GeV}$			

In Table 11, we compare our rate results with the results of some other approaches [37–42]. All calculations approximately agree on the rate of the decay $\Xi_{cc}^{++} \to \Xi_c^{\prime +} + \rho^+$, which is predicted to have a large branching ratio of $\sim 16\,\%$. In our calculation, this mode is predicted to have by far the largest branching ratio of the decays analyzed in this paper. As concerns the decay $\Xi_{cc}^{++} \to \Xi_c^+ + \pi^+$ discovered by the LHCb Collaboration [15], we find a branching ratio of $\mathcal{B}(\Xi_{cc}^{++} \to \Xi_c^+ \pi^+) = 0.70\%$ using the central value of the life time measurement in Reference [14]. The small value of the branching ratio results from a substantial cancellation of the tree and *W*–exchange contributions. The branching ratio is somewhat smaller than the branching ratio $\mathcal{B}(\Xi_{cc}^{++} \to \Sigma_c^{++} + \bar{K}^0) = 1.28\%$ calculated in Reference [43]. We think that the latter mode is more dominant in comparison with $\Xi_{cc}^{++} \to \Xi_c^+ \pi^+$. We predict a branching ratio considerably smaller than the range of branching fractions $(6.66 - 15.79)\,\%$ calculated in Reference [37]. In our opinion, the calculations done in Reference [37] involve generous approximations for the errors, which are hard to quantify.

Table 11. Comparison with other approaches. Abbreviation: M = NRQM, T = HQET.

Mode	Width (in 10^{-13} GeV)					
	GIKLT [22,43]	**DS** [37,39]	**JHL** [38]	**WYZ** [40]	**YJLLWZ** [41]	**KL** [42]
$\Xi_{cc}^{++} \to \Sigma_c^{++} + \bar{K}^0$	0.33					
$\Xi_{cc}^{++} \to \Sigma_c^{++} + \bar{K}^{*\,0}$	1.38					
$\Omega_{cc}^{+} \to \Xi_c^{\prime +} + \bar{K}^0$	0.15	0.31 (M) 0.59 (T)				
$\Omega_{cc}^{+} \to \Xi_c^{+} + \bar{K}^0$	0.95	0.68 (M) 1.08 (T)				
$\Omega_{cc}^{+} \to \Xi_c^{\prime +} + \bar{K}^{*\,0}$	0.74		$2.64^{+2.72}_{-1.79}$			
$\Omega_{cc}^{+} \to \Xi_c^{+} + \bar{K}^{*\,0}$	0.62		$1.38^{+1.49}_{-0.95}$			
$\Xi_{cc}^{++} \to \Xi_c^{\prime +} + \pi^+$	0.82	1.40 (M) 1.93 (T)		1.10		
$\Xi_{cc}^{++} \to \Xi_c^{+} + \pi^+$	0.18	1.71 (M) 2.39 (T)		1.57	1.58	2.25
$\Xi_{cc}^{++} \to \Xi_c^{\prime +} + \rho^+$	4.27		$4.25^{+0.32}_{-0.19}$	4.12	3.82	
$\Xi_{cc}^{++} \to \Xi_c^{+} + \rho^+$	0.63		$4.11^{+1.37}_{-0.86}$	3.03	2.76	6.70

The only free parameter in our approach is the size parameter Λ_{cc} of the double heavy baryons, for which we have chosen $\Lambda_{cc} = 0.8675$ GeV in Tables 7–10. In order to estimate the uncertainty caused by the choice of the size parameter, we allow the size parameter to vary from 0.6 to 1.135 GeV. We evaluate the mean $\bar{\Gamma} = \sum \Gamma_i / N$ and the mean square deviation $\sigma^2 = \sum (\Gamma_i - \bar{\Gamma})^2 / N$. The results for $N = 5$ are shown in Table 12. The rate errors amount to 6–15%. Since the dependence of the rates on Λ_{cc} is nonlinear, the central values of the rates in Table 12 do not agree with the rate values in Tables 7–10.

Table 12. Estimating uncertainties in the decay widths.

Mode	Width (in 10^{-13} GeV)
$\Omega_{cc}^{+} \to \Xi_c^{\prime +} + \bar{K}^0$	0.14 ± 0.01
$\Omega_{cc}^{+} \to \Xi_c^{\prime +} + \bar{K}^{*0}$	0.72 ± 0.06
$\Omega_{cc}^{+} \to \Xi_c^{+} + \bar{K}^0$	0.87 ± 0.13
$\Omega_{cc}^{+} \to \Xi_c^{+} + \bar{K}^{*0}$	0.58 ± 0.07
$\Xi_{cc}^{++} \to \Xi_c^{\prime +} + \pi^+$	0.77 ± 0.05
$\Xi_{cc}^{++} \to \Xi_c^{\prime +} + \rho^+$	4.08 ± 0.29
$\Xi_{cc}^{++} \to \Xi_c^{+} + \pi^+$	0.16 ± 0.02
$\Xi_{cc}^{++} \to \Xi_c^{+} + \rho^+$	0.59 ± 0.04

8. Outlook

The discovery of the doubly charmed baryon Ξ_{cc}^{++} by the LHCb Collaboration [13,14] and the first observation of its two-body nonleptonic decay $\Xi_{cc}^{++} \to \Xi_c^{+} + \pi^+$ [15] provided strong encouragement for further theoretical analysis of the weak decays of doubly charmed baryons. As well known, such decays are described by the quark diagrams, which have several different topologies. One class of the diagrams having the so-called factorizing topology is easy to evaluate in almost model independent way, whereas another class with the internal W–exchange is extremely difficult to handle theoretically. In this lecture, we gave a basic introduction to the methods of how to calculate the relevant diagrams with any topologies in self-consistent way on the same basis. The theoretical background used for this purpose is the covariant constituent model previously developed in our papers. As the first step, we concentrated on the description of Cabibbo-favored nonleptonic two-body decays of the doubly charmed ground state baryons Ξ_{cc}^{++} and Ω_{cc}^{+} where we have limited our analysis to the $\frac{1}{2} \to \frac{1}{2} + P(V)$ decay channels. It would be straightforward to also include $\frac{1}{2} \to \frac{3}{2} + P(V)$ the nonleptonic decays in the future. In addition, the study could be extended to the description of singly and doubly suppressed Cabibbo decays, not only for doubly charmed baryon decays but also for singly charmed baryon decays.

Funding: This research was partly supported by the PRISMA+Cluster of Excellence (Mainz Uni.).

Acknowledgments: I would like to thank Thomas Gutsche, Jürgen Körner, Valery Lyubovitskij, Pietro Santorelli and Zhomart Tyulemissov for their collaboration in which the results discussed in this lecture have been obtained.

Conflicts of Interest: The author declares no conflict of interest.

References

1. Gell–Mann, M. A Schematic Model of Baryons and Mesons. *Phys. Lett.* **1964**, *8*, 214–215. [CrossRef]
2. Zweig, G. *An SU(3) Model for Strong Interaction Symmetry and Its Breaking*, Version 1; PREPRINT CERN-TH-401; 1964; pp. 1–26. Available online: inspirehep.net/record/11881/files/CM-P00042883.pdf (accessed on 6 January 2020).

3. Zweig, G. *An SU(3) Model for Strong Interaction Symmetry and Its Breaking*, Version 2; PREPRINT CERN-TH-412; 1964; pp. 1–68. Available online: https://cds.cern.ch/record/570209/files/CERN-TH-412.pdf (accessed on 6 January 2020).
4. Bjorken, J.D.; Glashow, S.L. Elementary Particles and SU(4). *Phys. Lett.* **1964**, *11*, 255–257. [CrossRef]
5. Glashow, S.L.; Iliopoulos, J.; Maiani, L. Weak Interactions with Lepton-Hadron Symmetry. *Phys. Rev. D* **1970**, *2*, 1285–1292. [CrossRef]
6. De Rujula, A.; Georgi, H.; Glashow, S.L. Hadron Masses in a Gauge Theory. *Phys. Rev. D* **1975**, *12*, 147–162. [CrossRef]
7. Körner, J.G.; Kramer, M.; Pirjol, D. Heavy baryons. *Prog. Part. Nucl. Phys.* **1994**, *33*, 787–868. [CrossRef]
8. Tanabashi, M.; Hagiwara, K.; Hikasa, K.; Nakamura, K.; Sumino, Y.; Takahashi, F.; Tanaka, J.; Agashe, K.; Aielli, G.; Amsler, C.; et al. Review of particle physics. *Phys. Rev. D* **2018**, *98*, 030001. [CrossRef]
9. Ablikim, M.; Achasov, M.N.; Ai, X.C.; Albayrak, O.; Albrecht, M.; Ambrose, D.J.; Amoroso, A.; An, F.F.; An, Q.; Bai, J.Z.; et al. Measurements of absolute hadronic branching fractions of Λ_c^+ baryon. *Phys. Rev. Lett.* **2016**, *116*, 052001. [CrossRef]
10. Li, Y.B.; Shen, C.P.; Yuan, C.Z.; Adachi, I.; Aihara, H.; Al Said, S.; Asner, D.M.; Aushev, T.; Ayad, R.; Badhrees, I.; et al. First, measurements of absolute branching fractions of the Ξ_c^0 baryon at Belle. *Phys. Rev. Lett.* **2019**, *122*, 082001. [CrossRef]
11. Li, Y.B.; Shen, C.P.; Adachi, I.; Ahn, J.K.; Aihara, H.; Al Said, S.; Asner, D. M.; Atmacan, H.; Aushev, T.; Ayad, R.; et al. First measurements of absolute branching fractions of the Ξ_c^+ baryon at Belle. *Phys. Rev. D* **2019**, *100*, no. 3, 031101. [CrossRef]
12. Ocherashvili, A.; Moinester, M.A.; Russ, J.; Engelfried, J.; Torres, I.; Akgun, U.; Alkhazov, G.; Amaro-Reyes, J.; Atamantchouk, A.G.; Ayan, A.S.; et al. Confirmation of the double charm baryon $\Xi_{cc}^+(3520)$ via its decay pD^+K^-. *Phys. Lett. B* **2005**, *628*, 18. [CrossRef]
13. Aaij, R.; Adeva, B.; Adinolfi, M.; Ajaltouni, Z.; Akar, S.; Albrecht, J.; Alessio, F.; Alexander, M.; Albero, A.A.; Ali, S.; et al. Observation of the doubly charmed baryon Ξ_{cc}^{++}. *Phys. Rev. Lett.* **2017**, *119*, 112001. [CrossRef] [PubMed]
14. Aaij, R.; Adeva, B.; Adinolfi, M.; Aidala, C.A.; Ajaltouni, Z.; Akar, S.; Albicocco, P.; Albrecht, J.; Alessio, F.; Alexander, M.; et al. Measurement of the lifetime of the doubly charmed baryon Ξ_{cc}^{++}. *Phys. Rev. Lett.* **2018**, *121*, 052002. [CrossRef] [PubMed]
15. Aaij, R.; Adeva, B; Adinolfi, M.; Aidala, C.A.; Ajaltouni, Z.; Akar, S.; Albicocco, P.; Albrecht, J.; Alessio, F.; Alexander, M.; et al. First, observation of the doubly charmed baryon decay $\Xi_{cc}^{++} \to \Xi_c^+\pi^+$. *Phys. Rev. Lett.* **2018**, *121*, 162002. [CrossRef] [PubMed]
16. Körner, J.G.; Krämer, M. Exclusive nonleptonic charm baryon decays. *Z. Phys. C* **1992**, *55*, 659. [CrossRef]
17. De Rujula, A.; Georgi, H.; Glashow, S.L. Vector Model of the Weak Interactions. *Phys. Rev. D* **1975**, *12*, 3589. [CrossRef]
18. Ebert, D.; Faustov, R.N.; Galkin, V.O.; Martynenko, A.P. Mass spectra of doubly heavy baryons in the relativistic quark model. *Phys. Rev. D* **2002**, *66*, 014008. [CrossRef]
19. Fleck, S.; Richard, J.M. Baryons with double charm. *Prog. Theor. Phys.* **1989**, *82*, 760. [CrossRef]
20. Karliner, M.; Rosner, J.L. Baryons with two heavy quarks: Masses, production, decays, and detection. *Phys. Rev. D* **2014**, *90*, 094007. [CrossRef]
21. Gutsche, T.; Ivanov, M.A.; Körner, J.G.; Lyubovitskij, V.E. Novel ideas in nonleptonic decays of double heavy baryons. *Particles* **2019**, *2*, 339–356. [CrossRef]
22. Gutsche, T.; Ivanov, M.A.; Körner, J.G.; Lyubovitskij, V.E.; Tyulemissov, Z. Ab initio three-loop calculation of the *W*-exchange contribution to nonleptonic decays of double charm baryons. *Phys. Rev. D* **2019**, *99*, 056013 [CrossRef]
23. Fayyazuddin and Riazuddin. *A Modern Introduction to Particle Physics*; World Scientific: Singapore, 1994; 656p.
24. Efimov, G.V.; Ivanov, M.A.; Lyubovitskij, V.E. Quark - diquark approximation of the three quark structure of baryons in the quark confinement model. *Z. Phys. C* **1990**, *47*, 583–594. [CrossRef]
25. Ioffe, B.L. On The Choice Of Quark Currents In The Qcd Sum Rules For Baryon Masses. *Z. Phys. C* **1983**, *18*, 67. [CrossRef]
26. Reinders, L.J.; Rubinstein, H.; Yazaki, S. Hadron Properties from QCD Sum Rules. *Phys. Rept.* **1985**, *127*, 1. [CrossRef]

27. Leibovich, A.K.; Ligeti, Z.; Stewart, I.W.; Wise, M.B.; Predictions for nonleptonic Lambda(b) and Theta(b) decays, *Phys. Lett. B* **2004**, *586*, 337. [CrossRef]
28. Ivanov, M.A.; Khomutenko, O.E.; Mizutani, T. Form-factors of semileptonic decays of heavy mesons in the quark confinement model. *Phys. Rev. D* **1992**, *46*, 3817. [CrossRef]
29. Ivanov, M.A.; Kalinovsky, Y.L.; Roberts, C.D. Survey of heavy meson observables. *Phys. Rev. D* **1999**, *60*, 034018. [CrossRef]
30. Ivanov, M.A.; Körner, J.G.; Tran, C.T. Exclusive decays $B \to \ell^- \bar{\nu}$ and $B \to D^{(*)} \ell^- \bar{\nu}$ in the covariant quark model. *Phys. Rev. D* **2015**, *92*, 114022 [CrossRef]
31. Branz, T.; Faessler, A.; Gutsche, T.; Ivanov, M.A.; Körner, J.G.; Lyubovitskij, V.E. Relativistic constituent quark model with infrared confinement. *Phys. Rev. D* **2010**, *81*, 034010. [CrossRef]
32. Vermaseren, J.A.M. The FORM project. *Nucl. Phys. Proc. Suppl.* **2008**, *183*, 19. [CrossRef]
33. Körner, J.G. Octet behaviour of single-particle matrix elements $< B'|H(W)|B >$ and $< M'|H(W)|M >$ using a weak current current quark Hamiltonian. *Nucl. Phys. B* **1971**, *25*, 282.
34. Pati, J.C.; Woo, C.H. Delta $I = 1/2$ rule with fermion quarks. *Phys. Rev. D* **1971**, *3*, 2920. [CrossRef]
35. Gutsche, T.; Ivanov, M.A.; Körner, J.G. Lyubovitskij, V.E.; Tyulemissov, Z. Analysis of the semileptonic and nonleptonic two-body decays of the double heavy charm baryon states Ξ_{cc}^{++}, Ξ_{cc}^{+} and Ω_{cc}^{+}. *Phys. Rev. D* **2019**, *100*, 114037. [CrossRef]
36. Gutsche, T.; Ivanov, M.A.; Körner, J.G.; Lyubovitskij, V.E.; Santorelli, P. Semileptonic decays $\Lambda_c^+ \to \Lambda \ell^+ \nu_\ell$ $(\ell = e, \mu)$ in the covariant quark model and comparison with the new absolute branching fraction measurements of Belle and BESIII. *Phys. Rev. D* **2016**, *93*, 034008. [CrossRef]
37. Sharma, N.; Dhir, R. Estimates of W–exchange contributions to Ξ_{cc} decays. *Phys. Rev. D* **2017**, *96*, 113006. [CrossRef]
38. Jiang, L.J.; He, B.; Li, R.H. Weak Decays of Doubly Heavy Baryons: $\mathcal{B}_{cc} \to \mathcal{B}_c V$. *Eur. Phys. J. C* **2018**, *78*, 961. [CrossRef]
39. Dhir, R.; Sharma, N. Weak decays of doubly heavy charm Ω_{cc}^{+} baryon. *Eur. Phys. J. C* **2018**, *78*, 743. [CrossRef]
40. Wang, W.; Yu, F.S.; Zhao, Z.X. Weak decays of doubly heavy baryons: The $1/2 \to 1/2$ case. *Eur. Phys. J. C* **2017**, *77*, 781. [CrossRef]
41. Yu, F. S.; Jiang, H.Y.; Li, R.H.; Lü, C.D.; Wang, W.; Zhao, Z.X. Discovery Potentials of Doubly Charmed Baryons. *Chin. Phys. C* **2018**, *42*, 051001. [CrossRef]
42. Kiselev, V.V.; Likhoded, A.K. Baryons with two heavy quarks. *Phys. Usp.* **2002**, *45*, 455. [CrossRef]
43. Gutsche, T.; Ivanov, M.A.; Körner, J.G.; Lyubovitskij, V.E. Decay chain information on the newly discovered double charm baryon state Ξ_{cc}^{++}. *Phys. Rev. D* **2017**, *96*, 054013. [CrossRef]